行政院國家科學委員會專題研究計畫　成果報告

子計畫一：光纖都會核心網路技術研究(3/3)

計畫類別：整合型計畫
計畫編號：NSC94-2213-E-009-016-
執行期間：94 年 08 月 01 日至 95 年 07 月 31 日
執行單位：國立交通大學資訊工程學系(所)

計畫主持人：楊啟瑞

計畫參與人員：羅志鵬、施汝霖、趙一芬、林士勛

報告類型：完整報告

處理方式：本計畫可公開查詢

中　華　民　國 95 年 10 月 27 日

行政院國家科學委員會專題研究計畫成果報告

光纖都會核心網路技術研究

Optical Metro Core Network Technology

計畫編號：NSC94-2213-E-009-016
執行期限： 94 年 8 月 1 日至 95 年 7 月 31 日

主持人：楊啟瑞　　國立交通大學資訊工程研究所

一、中文摘要

網際網路頻寬需求的成長以及全光波長分波多工(WDM)技術的改進，使得下一世代網路的設計與實作已經具有重大的改變。為了提供端點對端點的資料傳輸性能，共有三種不同層次的網路：廣域長途骨幹網路、都會核心網路以及區域接取網路。我們在這個子計畫已針對全光都會核心網路技術來探討。本計畫第一年我們已提出一套新的全光近屬封包交換技術(OCPS)，適用於以OCPS網狀架構為主的都會核心網路。此技術提倡並主張採用高度管理化的訊務控制與訊務工程技術，在次波長範圍內實現隨選頻寬。根據OCPS概念，我們也架構了一個全光IP-over-WDM網路實驗平台，稱之為OPSINET。OPSINET之服務品質叢聚控制技術亦藉由一套稱之為(ψ,τ)-封包排程器/流量控制器的服務品質強化訊務控制技術來實現。程式模擬結果顯示，相對於現存的全光叢集交換技術(OBS)，OCPS具有較優越的封包遺失表現。在計畫的第二年，我們提出了一套高效率的近似法來解決具備波長與光纖交換器之多重量度分波多工網路之路由與波長分配問題，此方法稱之為拉式鬆弛試誤法(LRH)。藉由亂數產生之網路與幾種為人熟知的大型網路來比較LRH與現存已實作出的方法，數值模擬結果顯示LRH於準確性以及計算時間複雜度上，皆優於現存方法，特別是在較大型的網路之表現上。計畫最後一年我們設計並實驗一個高性能的全光封包交換都會WDM環狀網路(HOPSMAN)。配置新的媒體存取控制技術，HOPSMAN具有較優越的頻寬效率、接取延遲、公平性以及大量突發訊務適應性。

關鍵詞：波長分波多工(WDM)、全光封包交換(OPS)、全光叢集交換(OBS)、服務品質保證(QoS)、多重粗細粒度交換能力、路由與波長分配(RWA)、組合性最佳化問題、拉式鬆弛法、媒體存取控制(MAC)、都會網路(MAN)。

二、英文摘要

The ever-growing demand for Internet bandwidth and recent advances in optical Wavelength Division Multiplexing (WDM) technologies brings about fundamental changes in the design and implementation of the next generation networks. To support end-to-end data transport, there are three types of networks: wide-area long-haul backbone network, metropolitan core network, and local and access networks. In this subproject, we focus on the optical metro core network technologies. In the first year, we have proposed a new Optical Coarse Packet Switching (OCPS) paradigm for OCPS mesh-based metro core networks. OCPS advocates the enforcement of manageable traffic control and engineering to realize bandwidth-on-demand on sub-wavelength basis. Based on OCPS, we have constructed an experimental optical IP-over-WDM network testbed, referred to as OPSINET. The QoS burstification control of OPSINET is performed by a QoS-enhanced traffic control scheme, called (ψ,τ)-Scheduler/Shaper. Simulation results demonstrated that OCPS is shown to achieve invariably superior packet loss probability than the existing Optical Burst Switching (OBS) paradigm. In the second year, we have proposed an efficient approximation approach, called Lagrangean Relaxation with Heuristics (LRH), aimed to resolve Routing and Wavelength Assignment (RWA) in multi-granularity WDM networks particularly with lambda and fiber switches. Compare between LRH and an existing practical approach via experiments over randomly generated and several well-known large sized networks. Numerical results demonstrate that LRH outperforms the existing approach in both accuracy and computational time complexity, particularly for larger sized networks. In the last year, we present the design and experimentation of a high-performance optical packet-switched metro WDM ring network (HOPSMAN). Equipped with

novel medium access control, HOPSMAN achieves superior bandwidth efficiency, access delay, fairness, and bursty traffic adaptation.

Keywords: Wavelength Division Multiplexing (WDM), Optical Packet Switching (OPS), Optical Burst Switching (OBS), Quality-of-Service (QoS), Multi-granularity switching capabilities, Routing and Wavelength Assignment (RWA), Combinatorial optimization problem, Lagrangean relaxation, Medium Access Control (MAC), Metropolitan Area Network (MAN).

三、計畫緣由與目的

The ever-growing demand for Internet bandwidth and recent advances in optical Wavelength Division Multiplexing (WDM) [1] technologies brings about fundamental changes in the design and implementation of the next generation networks. Even though the optical long-haul Internet has been designed to foster the current traffic demand and bandwidth growth trend, two critical bottlenecks are still present in network chains. The first one is the so-called last mile, or access networks, which provide bandwidth directly to end-users. The other one that behaves as transitional bandwidth distributors between the optical Internet and access networks is the core of Metropolitan Area Networks (MANs) [2], referred to as metro core network. Long-haul optical Internet is based on a mesh topology, and follows the Optical Circuit Switching (OCS) paradigm by making relatively static WDM channel utilization. As opposed to it, optical metro core networks are based on mesh, ring, or bus topologies. Prevailing examples of mesh and ring networks are packet-over-WDM (PoW), and packet-over-SONET (PoS), respectively.

Unlike long-haul backbone networks, metro networks exhibit highly dynamic traffic demand, rendering static WDM channel utilization completely infeasible. Accordingly, while mesh-based networks require fine-grained packet-switched-based on-demand channel allocation, namely Optical Packet Switching (OPS) [3-6], ring/bus networks require versatile Medium Access Control (MAC) schemes to assure efficient bandwidth allocation and various Quality-of-Service (QoS) guarantees. Unfortunately, the OPS technique currently faces some technological limitations, such as the lack of optical signal processing and optical buffer, and large switching overhead. To alleviate these limitations, much research work has been devoted to seeking for promising OPS alternatives. Among them, Optical Burst Switching (OBS) [7-12] has been considered a promising candidate, however only suitable for long-haul backbone networks. Moreover, for ring/bus metro networks, most existing MAC schemes either discount the existence of wavelengths, or disregard QoS guarantees.

During this three-year project, we have designed, analyzed, and constructed of PoW mesh/ring metro networks. In the first year, we focus on the mesh-topology line of work. We have proposed a new Optical Coarse Packet Switching (OCPS) [13,14] paradigm for OCPS mesh-based metro core networks. Combining the best of OPS and OBS, OCPS advocates the enforcement of manageable traffic control and engineering to realize bandwidth-on-demand on sub-wavelength basis while circumventing OPS limitations. Based on OCPS, we have constructed an experimental optical IP-over-WDM network testbed, referred to as OPSINET. OPSINET consists of three types of nodes-edge routers, optical lambda/fiber switches (OXCs), and Optical Label Switched Routers (OLSRs). To facilitate traffic engineering, OPSINET is augmented with an out-of-band Generalized Multiprotocol Label Switching (GMPLS) [15] control network. In sequel, we focus on QoS burstification control of OPSINET.

The QoS burstification control of OPSINET is performed by a QoS-enhanced traffic control scheme, called (ψ,τ)-Scheduler/Shaper, where ψ and τ are the maximum burst size (packet count) and maximum burst assembly time, respectively. Essentially, (ψ,τ)-Scheduler/Shaper is a dual-purpose scheme. It is a scheduler for packets, abbreviated as **(ψ,τ)-Scheduler**, which performs the scheduling of different delay class packets into back-to-back bursts. On the other hand, it is a shaper for bursts, referred to as **(ψ,τ)-Shaper**, which determines the sizes and departure times of bursts.

To provide delay class differentiation, for IP packet flows designated with delay-associated weights, (ψ,τ)-Scheduler performs packet scheduling and assembly into bursts based on their weights and a *virtual window* of size ψ. The Scheduler exerts simple FIFO service within the window and assures weight-proportional service at the window boundary. The scheme, as will be shown, provides different classes of 99% delay bound guarantees. To provide loss class differentiation, (ψ,τ)-Shaper facilitates traffic shaping with a larger burst size (ψ) assigned to a higher

priority class. Then, we conduct network-wide simulations to draw loss performance comparisons between OCPS and JET-based OBS [8]. Simulation results demonstrated that, due to the near-far problem [16], OBS undergoes several orders of magnitude increase in packet loss probability for Class *H* traffic particularly under a smaller burst size. As opposed to OBS, the in-band-controlled-based OCPS network was shown to provide invariably superior packet loss performance for a high priority traffic class, enabling effective facilitation of loss class differentiation.

In the second year, we focus on the Routing and Wavelength Assignment (RWA) problem [18,19] in multi-granularity WDM networks. With advances in optical Wavelength Division Multiplexing (WDM) technologies and its potential of providing virtually unlimited bandwidth, optical WDM networks have been widely recognized as the dominant transport infrastructure for future Internet backbone networks. To maintain high scalability and flexibility at low cost, WDM networks often include switching devices with different wavelength conversion powers [20,18] (e.g., no, limited- or full-range), and multi-granularity switching capability [21,22]. In particular, examples of Multi-Granularity Optical crossconnects (MG-OXCs) include switching on a single lambda, a waveband (i.e., multiple lambdas), an entire fiber, or a combination of above.

One major traffic engineering challenge in such WDM networks has been the Routing and Wavelength Assignment (RWA) problem. The problem deals with routing and wavelength assignment between source and destination nodes subject to the wavelength-continuity constraint [23] in the absence of wavelength converters. It has been shown that RWA is an NP-complete problem [23]. Numerous approximation algorithms [18,19] have been proposed with the aim of balancing the trade-off between accuracy and computational time complexity. In general, some algorithms [24,25] focused on the problem in the presence of sparse, limited, or full-range wavelength converters. Some others made an effort to either reduce computational complexity by solving the routing and wavelength assignment sub-problems separately [23], or increase accuracy by considering the two sub-problems [26] jointly. However, with the multi-granularity switching capability taken into consideration, most existing algorithms become functionally or economically unviable.

Our aim is to resolve the RWA problem in multi-granularity WDM networks particularly with Fiber Switch Capable (FSC-OXC) and Lambda Switch Capable (LSC-OXC) devices. It is worth mentioning that, an MG-OXC node is logically identical to an individual FSC-OXC node in conjunction with an external separated LSC-OXC node. For ease of illustration, we adopt the separated node form throughout the rest of the report. The problem is in short referred to as RWA^{+}.

We have resolved a RWA^{+} problem using the LRH method, which is a Lagrangean Relaxation based approach augmented with an efficient primal heuristic algorithm. With the aid of generated Lagrangean multipliers and lower bound indexes, the primal heuristic algorithm of LRH achieves a near-optimal upper-bound solution. A performance study delineated that the performance trade-off between accuracy and convergence speed can be manipulated via adjusting the Quiescence Threshold parameter in the algorithm. We have drawn comparisons of accuracy and computation time between LRH and the Linear Programming Relaxation (LPR)-based method, under three random networks. Experimental results demonstrated that, particularly for small to medium sized networks, the LRH approach using a termination requirement profoundly outperforms the LPR method and fixed-iteration-based LRH, in both accuracy and computational time complexity. Furthermore, for large sized networks, i.e., the USA and ARPA networks, numerical results showed that LRH achieves a near optimal solution within acceptable computation time. The above numerical results justify that the LRH approach can be used as a dynamic RWA^{+} algorithm for small to medium sized networks, and as a static RWA^{+} algorithm for large sized networks.

In the last year, we center on the design and experimentation of a high-performance MAC schemes achieving superior bandwidth access efficiency and different QoS guarantees in the ring topology. The future optical Metropolitan Area Networks (MANs) are expected to employ optical packet switching to cost-effectively support a wide range of heterogeneous traffic with different time-varying and high bandwidth demand. Optical Wavelength Division Multiplexing (WDM) has been highly successful in providing very high capacity in the backbone of the Internet. SONET has provided reliable circuit switched data transfer within

metropolitan areas, as well as data transfer from local networks to the backbone. According to the increasing portion of bursty data and multimedia traffic, the design focus of the networks is an efficient, flexible, and reliable optical packet switched for metro area networks.

Network nodes require dynamic capability to access a ring network flexibly and effectively. Nodes are generally equipped with tunable transmitters and tunable receivers [33-36]. Some networks adopt fixed transmitter and receiver arrays to achieve this objective [35,37,[38]. Advances in fast tunable lasers suggest that laser tuning times within several nano-seconds are commercially available, enabling fast and dynamic access to network resources. A Tunable Transmitter - Fixed Receiver (TT-FR) based bi-directional WDM ring network [33] has been implemented. The DQBR MAC (modified from IEEE 802.16 DQDB) exhibits various performance benefits, including high utilization and fairness, but requires a lot of counters to monitor the network status, leading to scalability problems. Additionally, their prototype network still suffers from the fairness problem while the traffic load exceeds 0.7.

An experimental ring network that uses low-cost commercial available components was demonstrated in [35]. The MAC protocol is based on the synchronous round robin (SRR) strategy. The latest version of SRR [36] combines TDMA, tokens and slot reservations to achieve high utilization and guarantee fairness. However, the MAC is too complex for most practical conditions.

DAVID is a major project for optical packet-switched MAN and WAN networks [34]. A DAVID metro network comprises several single fiber rings interconnected via a hub node. Since the hub exchanges packets among rings directly in the optical domain, careful slot reservation is necessary to achieve a feasible wavelength-to-wavelength permutation. DAVID is based on TT-TR architecture. Each node has an SOA-based slot eraser, enabling high slot reuse at the expense of prohibitive system cost.

The number of nodes in the network equals the number of required wavelengths in all the above architectures, making them hard to scale up. To overcome the problem, a FT-FR4 architecture [[38] has been proposed that the number of network nodes can exceed the number of the required wavelengths. Although capable of significantly enhancing the network performance, the proposed destination stripping scheme still suffers the unfairness problem from the proposed MAC.

In this work, we aim at the design and experimentation of an optical packet-switched metro WDM ring network (HOPSMAN), capable of achieving high cost-effectiveness, architecture scalability, and superior Medium Access Control (MAC) performance on bandwidth utilization, access delay, fairness, and bursty traffic adaptation.

The remainder of this report is organized as follows. In Section 4.1, we present the (ψ,τ)-Scheduler/Shaper design and performance comparison. In Section 4.2, we present the LRH approach and its primal heuristic algorithm to resolve RWA problem. In Section 4.3, we demonstrate the HOPSMAN network design. Finally, concluding remarks are made in Section 4.4.

四、成果與討論

4.1 (ψ,τ)-Scheduler/Shaper

4.1.1 Architecture and Design

In any ingress node, incoming packets (see Figure 1(a)) are first classified on the basis of their destination, loss and delay classes. Packets belonging to the same destination and loss class are assembled into a burst. Thus, a burst may contain packets belonging to different delay classes. In the figure, we assume there are *M* destination/loss classes and *N* delay classes in the system. For any one of *M* destination/loss classes, say class *k*, packets of flows belonging to *N* different delay classes are assembled into bursts through (ψ,τ)-Scheduler/Shaper$_k$ according to their pre-assigned delay-associated weights. Departing bursts from any (ψ,τ)-Scheduler/Shaper are optically transmitted, and forwarded via their corresponding, pre-established OLSP.

Essentially, (ψ,τ)-Scheduler/Shaper is a dual-purpose scheme. It is a scheduler for packets, abbreviated as **(ψ,τ)-Scheduler**, which performs the scheduling of different delay class packets into back-to-back bursts. On the other hand, it is a shaper for bursts, referred to as **(ψ,τ)-Shaper**, which determines the sizes and departure times of bursts.

In the (ψ,τ)-Scheduler system, each delay class is associated with a per-determined weight. A higher delay priority class is given a greater weight, which corresponds to a more stringent delay bound

requirement. In addition, we assume all packets are of fixed size of one unit. Generally, (ψ,τ)-Scheduler performs scheduling of packets in accordance with their weights and a *virtual window* of size ψ. The weight of a class corresponds to the maximum number of packets of the class that can be accommodated in a window, or burst in this case. Such window-based scheduling allows simple FIFO service within the window and assures weight-proportional service at the window boundary. In the sequel, we present the design and algorithm, followed by the specification of the stepwise service curve from which the guaranteed delay bound can be obtained.

Upon arriving, packets of different classes are sequentially inserted in a sequence of virtual windows. The window size, which is set as the maximum burst size, ψ, together with the weight (w) of a class, determines the maximum number of packets (i.e., quotas) from this class that can be allocated in a window. For a class, if there are sufficient quotas, its new packets are sequentially placed in the current window in a FIFO manner. Otherwise, its packets are placed in an upward window in accordance to the total accumulated quotas. A burst is formed and departs when the burst size reaches ψ or the Burst Assembly Timer (BATr) (set as τ initially) expires. For convenience, class weights are normalized to the window size. Namely, $\sum w_i = \psi$, where w_i is the normalized weight of class i.

The operation of (ψ,τ)-Scheduler is explained via a simple example illustrated in Figure 1(c). For ease of illustration, the packet size is assumed fixed. FCFS burstification (Figure 1(b)) simply assembles the first six arriving packets into a burst. As for (ψ,τ)-Scheduler, upon the arrivals of packets B_1 to B_4, due to the allowance of only two packets (w_B=2) in a window for flow B, packets B_3 and B_4 are placed in the next window. Next, packet C_1 arrives and is sequentially placed in the first window due to sufficient quota. At the end, if there is no further packet arriving, the last burst with only four packets (B_5, C_3, A_7, A_8) is transmitted after BATr expires.

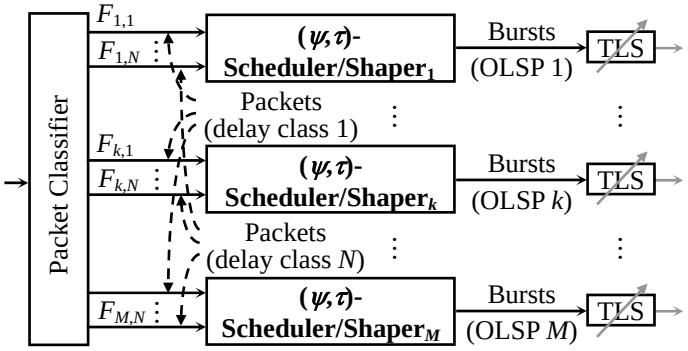

Legend:
$F_{d,y}$: Packet flow of destination/loss class d and of delay class y;
OLSP : Optical Label Switched Path;
TLS : Tunable Laser Source;

(a) System architecture

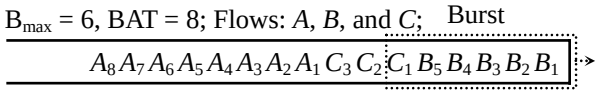

(b) FCFS-based burstification

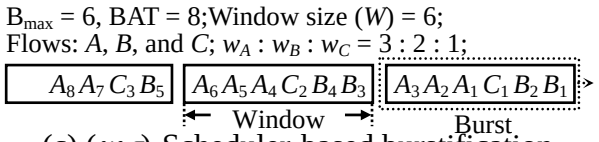

(c) (ψ,τ)-Scheduler-based burstification

Figure 1. (ψ,τ)-Scheduler architecture and design concept.

4.1.2 Delay QoS Provision

We seek stochastic delay performance metrics to the effectiveness of the weight-based scheduling on delay QoS provisioning. To this end, we carried out event-based simulations in which the mean packet delay and 99% delay bound (in units of slots) were measured. In the simulations, we have four delay classes (C1-C4), with the weights set as 10, 6, 5, and 4 (or 40, 24, 20, and 16, normalized with respect to ψ = 100). The system is served by a wavelength in a capacity of one 60-byte packet per slot time. Each of these four classes generate an equal amount of traffic based on a two-state (H and L) Markov Modulated Bernoulli Process (MMBP). In the MMBP, the probability of switching from state H (L) to L (H) is equal to $\alpha = 0.225$ ($\beta = 0.025$), and the probability of having one packet arrival during state H (L) is equal to $\bar{L}$ ($\bar{L}/6$), under an offered load, $\bar{L}$. Accordingly, the burstiness of traffic is B = 4. To draw a comparison, a FIFO system was also experimented. Simulations are terminated after reaching 95% confidence interval. Simulation results are plotted in Figures 2 and 3.

We observe from Figure 2 that both mean delay and 99% delay bound of all classes increase with the offered load. Superior to the FIFO system that undergoes long delay/bound at high loads, (ψ,τ)-Scheduler invariably assures low delay/bound for high priority classes (e.g., C1 and C2) at a cost of increased delay/bound for low priority classes (e.g., C4). In Figure 3, we illustrate how the weight of a

class can be adjusted to meet its delay/bound requirements. For example, as shown in Figure 3(b), to meet a 99% delay bound guarantee of 200 slots for class $C1$, the weight of $C1$ must be greater than 7, given the weights of three other classes of 6, 5, and 4, respectively.

For clarity purposes, we highlight the operation of (ψ,τ)-Shaper, particularly the BATr part of the system in the sequel. A burst of size ψ is generated and transmitted if the total number of packets reaches ψ before the burst assembly time exceeds τ. Otherwise, a burst of size less than ψ is generated when BATr expires. The BATr is initialized as the τ value when it is *activated* or *reset*. The BATr is activated when the system is changed from being idle to busy due to new packet arrivals. The BATr is immediately *reset* when a burst departs leaving behind a non-empty queue.

4.1.3 Loss QoS Performance Comparison

In this section, we demonstrate the performance of (ψ,τ)-Shaper on loss QoS performance comparison between the OCPS and the JET-based OBS [8] networks. Rather than considering one single switching node, we have simulated an entire optical network with QoS burst truncation and full wavelength conversion capabilities equipped in each switching node. The network we used in the experiment is the well-known ARPANET network [17] with 24 nodes and 48 links, in which 14 nodes are randomly selected as edge nodes. OLSP routing is subject to load balance of the network. Each link has up to 100 wavelengths, transmitting at 1 Gb/s, or one 60-byte packet per slot of duration 0.48μs. In simulations, departing bursts from ingress nodes can be served by any free wavelength, though, only after the previous burst has been fully transmitted.

In simulations, we generate packets according to

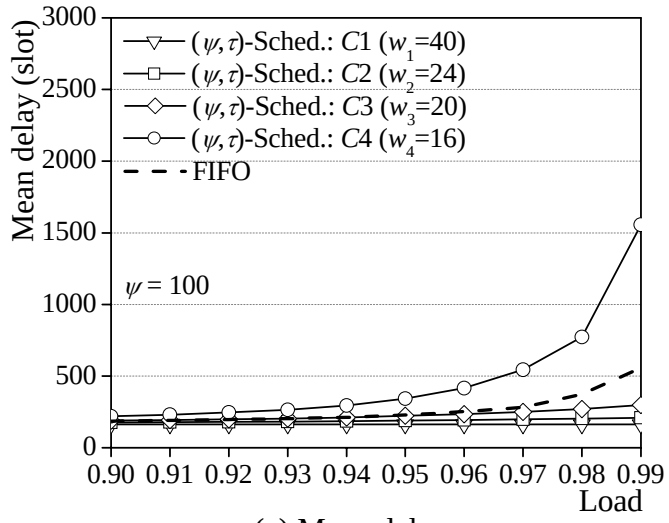

(a) Mean delay

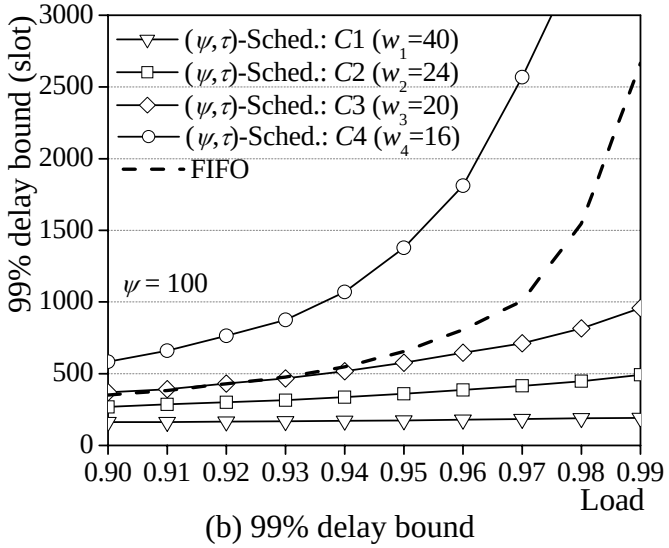

(b) 99% delay bound

Figure 2. Delay QoS provision under various loads.

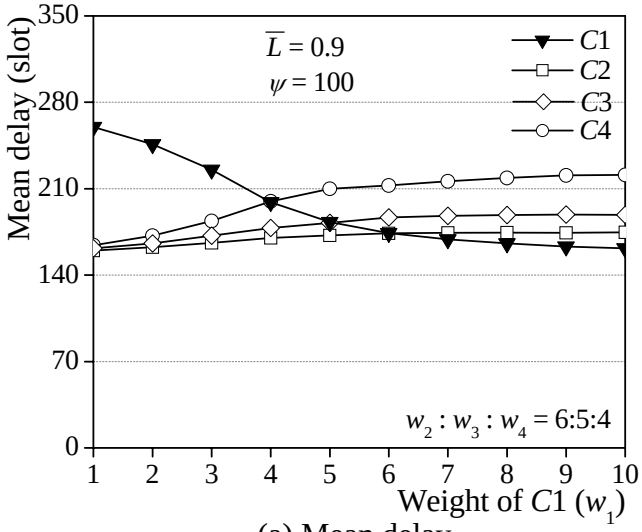

(a) Mean delay

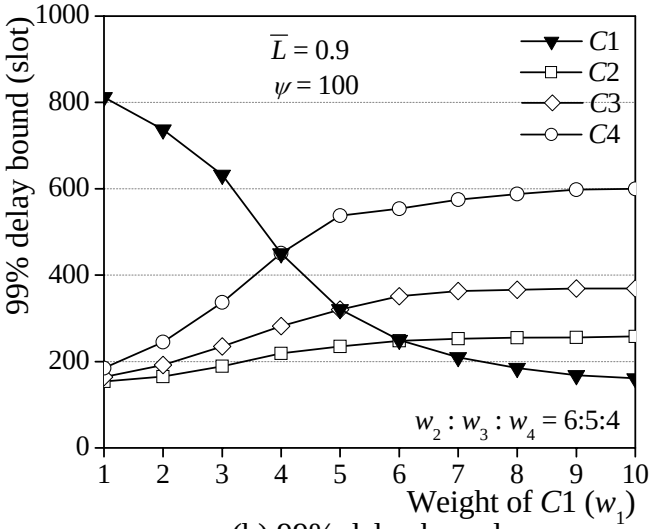

(b) 99% delay bound

Figure 3. Delay QoS provision via the weight adjustment.

the MMBP with $\alpha = 0.225$, $\beta = 0.025$, and the batch size in both *H* and *L* states being uniformly distributed between 1 and 9. For a given load ($\bar{L}$), traffic burstiness (*B*) is then uniquely determined by λ_H. The probability that a packet arrives at each slot is equal to the mean load ($\bar{L}$), yielding a total offered load of $W \cdot \bar{L}$, where *W* is the number of wavelengths. Simulations are terminated after reaching 95% confidence interval.

To examine the traffic shaping effect, we draw a comparison of burst loss probability between the baseline and OCPS networks. Simulation results are plotted in Figure 4. Compared with the baseline no-shaping network under MMBP arrivals, the OCPS network achieves more than five orders of magnitude reduction in burst loss probability under *W*=50, ψ =100, and $\bar{L}$ = 0.8 and below. Compared to smooth Binomial arrivals, the OCPS network with traffic shaping still yields several orders of magnitude improvement in burst loss probability. As shown in Figure 4(b), we discover that the improvement of loss probability is even more compelling in the presence of a large number of wavelengths (*W*=100) due to higher statistical multiplexing gain.

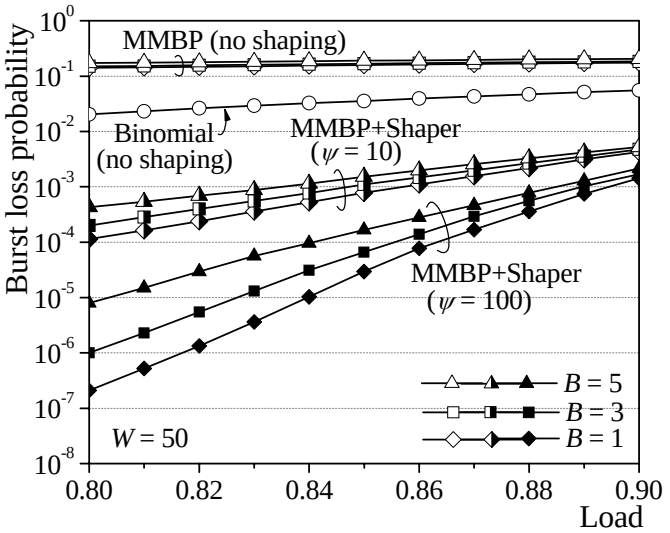

(a) *W*=50

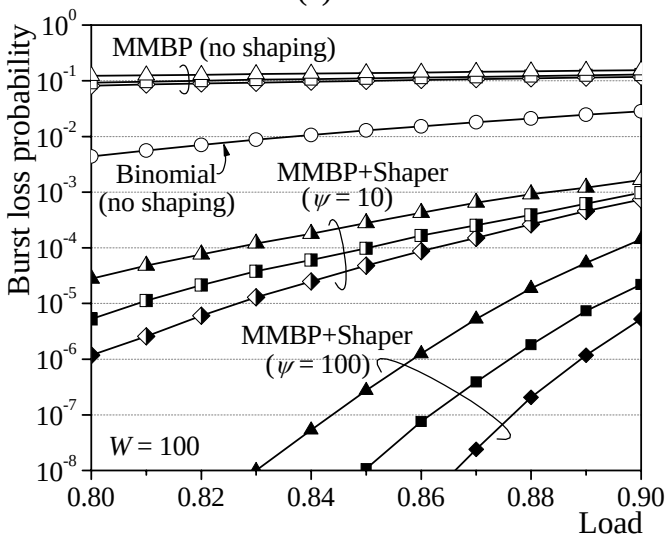

(b) *W*=100

Figure 4. Traffic shaping effect: a comparison between the OCPS and baseline networks.

As was mentioned, owing to the near-far problem and header-payload decoupling design, a JET-based OBS network supports *restricted* QoS burst truncation, resulting in loss performance degradation for high priority traffic classes. In this sub-section, we focus on this issue by making a comparison of packet loss probability between the OCPS and JET-based OBS networks. We carried out simulations on the 24-node ARPANET network in which three traffic classes (Classes *H*, *M*, and *L*) were adopted. In simulations, each ingress node generates a total of 39 connections (3 classes for each of 13 destination nodes) that follow different load-balancing OLSPs. For ease of comparison, we use the same burst size for all three classes during burstification, namely $\psi_H = \psi_M = \psi_L$.

For OCPS networks, we conduct QoS burst truncation in switching nodes on priority plus least-harm-preemption bases. For OBS networks, the offset time assigned to a burst is the total control packet processing time (path-dependent) plus the extra delay $x \cdot T$, where *T* is the maximum burst transmission time (e.g., 48μs for ψ=100), and *x* is (6,3,0), (4,2,0), or (2,1,0) for Classes (*H*, *M*, *L*), respectively. Notice that, in the OBS work reported in [8], the burst length is assumed exponentially distributed, and *T* is assigned as the mean burst length. It thus requires a large offset time difference between any two adjacent classes, such as (6,3,0), to meet 95 percent of traffic isolation degree. In our simulations, we apply the same timer (τ) and threshold (ψ) combined scheme to packet burstification for the OBS network. As a result, with *T* given as the maximum burst transmission time, all three above extra-delay settings, namely (6,3,0), (4,2,0), and (2,1,0), achieves 100 percent of traffic isolation degree. In addition, the header processing time (δ) at each switching node is assumed fixed. Finally, we employ restricted QoS burst truncation during contention for the OBS network. Specifically, truncation of bursts is also accomplished on priority plus least-harm-preemption bases, but restricted to those bursts whose control

packets have not yet departed from the switch. Simulations results are displayed in Figure 5.

We draw comparisons of packet loss probabilities of all three traffic classes between the OCPS and three variants of OBS networks using three extra-delay settings, respectively, under four cases set by two burst sizes (ψ= 25, 100) and two header processing times (δ= 9.6μs, 48μs). First, we observe from the figure that the OCPS and OBS networks provide typically the same grade of loss performance for Classes *M* and *L* under all four cases. Significantly, we discover that, compared to OCPS as shown in Figures 5(a) and (c), OBS undergoes several orders of magnitude deterioration in packet loss performance for Class *H* traffic particularly under a smaller burst size, i.e., $\psi_H=\psi_M=\psi_L$=25. Among the three OBS variants, OBS(2,1,0) using the smallest extra offset time difference (=*T*) invariably suffers from the poorest packet loss probability. Such performance degradation is caused by the near-far problem that exacerbates under a smaller burst size, a larger header processing time, and/or a smaller extra offset time difference. Under any of the conditions, the offset time of a Class-*H* burst is more likely to be smaller than that of a Class-*M* or Class-*L* burst, resulting in failing to make earlier wavelength reservation for the burst. This fact accounts for the poorest performance for Class *H* taking place under $\psi_H=\psi_M=\psi_L$=25 and δ=48μs, as shown in Figure 5(a). As the burst size increases and the processing time decreases, as shown in Figures 5(b), (c) and (d), the near-far problem is relaxed, yielding noticeable performance improvement for Class *H* in OBS networks. As

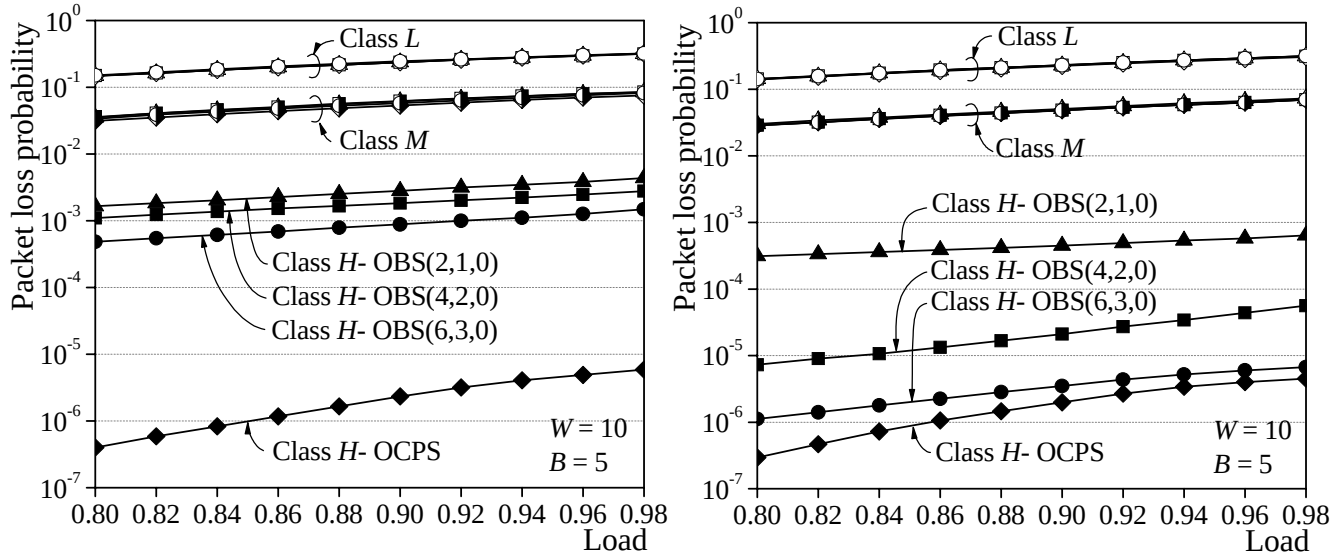

(a) $\psi_H=\psi_M=\psi_L$=25 and δ=48μs (b) $\psi_H=\psi_M=\psi_L$=100 and δ=48μs

(c) $\psi_H=\psi_M=\psi_L$=25 and δ=9.6μs (d) $\psi_H=\psi_M=\psi_L$=100 and δ=9.6μs

Figure 5. OCPS and OBS loss performance comparison.

opposed to OBS, the in-band-controlled-based OCPS networks are shown to provide invariably superior packet loss probability for Class *H* traffic, enabling effective facilitation of loss class differentiation.

4.2 Routing and Wavelength Assignment

4.2.1 RWA$^+$: Problem Formulation

The RWA$^+$ problem is formulated as a linear integer problem stated as follows. Given a physical topology (with FSC-OXCs and LSC-OXCs) and available wavelengths on each link, and requested lightpath demands between all source-destination pairs, determine the routes and wavelengths of lightpaths, such that the maximum number of lightpaths on the most congested link is minimized, subject to the wavelength continuity constraint. For ease of illustration, we assume in the sequel that the number of available wavelengths on each link is the same.

Due to the existence of FSC nodes, a graph transformation is first required. For each FSC node with *K* input (and output) fibers, it is replaced by a bipartite subgraph with *K* phantom nodes connecting to input fibers, and another *K* phantom nodes connecting to output fibers. Besides, there are additional *K*×*K* phantom links connecting the 2*K* phantom nodes. These phantom links describe possible configuration combinations inside an FSC node. For ease of description, we summarize the notation used in the formulation as follows.

Let N^F denote the set of FSC nodes in the network; N^L denote the set of LSC nodes in the network; L denote the set of physical optical links; L^F denote the set of phantom links within FSC nodes; V_n^{in} denote the set of phantom input nodes for node *n*; V_n^{out} denote the set of phantom output nodes for node *n*; *W* denote the set of available wavelengths on each link; (assumed to be the same for simplicity); *S* denote the set of source-destination (SD) pairs requesting lightpath set-up; S_n denote the set of SD pairs where node n is the source node; P_{sd} denote candidate path set for SD pair *sd*; y_{sd} denote lightpath demand for SD pair *sd*; δ_{pl} =1, if path *p* includes link *l*; =0, otherwise; and σ_{lv} =1, if link *l* is incident to node *v*; =0, otherwise; For outputs decision variables, α denote most congested link utilization (lightpath no./|W|); x_{pw}=1, if lightpath p uses wavelength w; =0, otherwise; and z_l=1, if phantom link *l* is selected; =0, otherwise. The formulation is given as

Problem (P):

min α

subject to

$$\sum_{sd\in S}\sum_{p\in P_{sd}}\sum_{w\in W} x_{pw}\delta_{pl} \le \alpha|W| \qquad \forall l\in L \quad (1)$$

$$\sum_{p\in P_{sd}}\sum_{w\in W} x_{pw} = y_{sd} \qquad \forall sd\in S \quad (2)$$

$$\sum_{sd\in S}\sum_{p\in P_{sd}} x_{pw}\delta_{pl} \le 1 \qquad \forall l\in L, w\in W \quad (3)$$

$$\sum_{sd\in S}\sum_{p\in P_{sd}} x_{pw}\delta_{pl} \le z_l \qquad \forall l\in L^F, w\in W \quad (4)$$

$$\sum_{l\in L^F} z_l\sigma_{lv} = 1 \qquad \forall v\in V_n^{in}, n\in N^F \quad (5)$$

$$\sum_{l\in L^F} z_l\sigma_{lv} = 1 \qquad \forall v\in V_n^{out}, n\in N^F \quad (6)$$

$$x_{pw} = 0 \text{ or } 1 \qquad \forall p\in P_{sd}, sd\in S, w\in W \quad (7)$$

$$0 \le \alpha \le 1 \quad (8)$$

$$z_l = 0 \text{ or } 1 \qquad \forall l\in L^F \quad (9)$$

$$\sum_{sd\in S_n}\sum_{p\in P_{sd}} x_{pw}\delta_{pl} \le 1 \qquad \forall n\in N^L, l\in L\cup L^F, w\in W \quad (10)$$

The objective function is to minimize the highest utilization (α), namely the utilization on the most congested fiber link with the maximum number of lightpaths passing through.

The problem is NP-complete [23], and is unlikely to obtain an exact solution for realistic networks in real-time. The problem is approximated using the LRH approach presented in the next section.

4.2.2 The Lagrangean Relaxation with Heuristics (LRH) Approach

The Lagrangean relaxation (LR) method [28,29,30] is used to derive the lower and upper bounds of the solution. First for the lower bound, Problem (P) is approximated by a Lagrangean relaxation problem, called Dual_P, by relaxing Constraints (1), (3), and (4). The objective function is accordingly reformed as

Problem (Dual_P):

$$Z_{dual}(\rho)=\min\left[\begin{array}{l}(1-\sum_{l\in L} s_l|W|)\alpha \\ +\sum_{sd\in S}\sum_{p\in P_{sd}}\sum_{w\in W}(\sum_{l\in L}(s_l+q_{lw})\delta_{pl}+\sum_{l\in L^F} r_{lw}\delta_{pl})x_{pw} \\ -\sum_{l\in L^F}\sum_{w\in W} r_{lw}z_l-\sum_{l\in L}\sum_{w\in W} q_{lw}\end{array}\right]$$

subject to Constraints (2), (5), (6), (7), (8), (9) and (10) where $\boldsymbol{\rho}=(\boldsymbol{q},\boldsymbol{r},\boldsymbol{s})$ is the non-negative Lagrangean multiplier vector. By separating decision variable α, and decision variable vectors, $\boldsymbol{x}$, $\boldsymbol{z}$, Problem (Dual_P) can be decomposed into three independent polynomial-bound sub-problems that can be efficiently solved. According to the weak Lagrangean

duality theorem [30], Z_{dual} is a lower bound of the original Problem (P) for any non-negative Lagrangean multiplier vector $\boldsymbol{\rho}$= ($\boldsymbol{q}$, $\boldsymbol{r}$, $\boldsymbol{s}$) ≥ 0. Clearly, we determine the greatest lower bound, i.e., $Z_{LB} = \max_{\rho>0} Z_{dual}(\rho)$, which can be solved by the subgradient method. Specifically, in the kth interation of the subgradient optimization procedure, Lagrangean multiplier vector $\boldsymbol{\rho}$ is updated as $\rho_{k+1} = \rho_k + \theta_k b_k$, where θ_k is the step size, determined by $\theta_k = \lambda_k (UB - Z_{dual}(\rho_k)) / \|b_k\|^2$, in which λ_k is the step size coefficient, *UB* is the current achievable least upper bound obtained from the heuristic algorithm described next, and b_k is a subgradient of $Z_{dual}(\rho)$ with vector size $|L+LW + L^F W|$.

The primal heuristic algorithm in the LRH approach is used to find an updated upper bound *ub*. Similar to the lower bound case, if the new upper bound (*ub*) is tighter (smaller) than the current best achievable upper bound (UB), the new upper bound is designated as the UB.

At the end of the computation, the costs of those links associated with the selected wavelengths/paths are set to ∞ to prevent the links from being considered by other upcoming iterations. If the number of wavelengths (lightpaths) used on a link is greater than the current tightest lower bound multiplied by $|W|$, indicating potential congestion, the cost of the link is then scaled by multiplying by a constant, referred to as the penalty term. This is to avoid further lightpath set-up through this link. The process repeats until either the lightpath demands of all SD pairs are satisfied (i.e., feasible), or there is no remaining resource (i.e., infeasible) in the network.

4.2.3 Performance Comparisons

We have carried out a performance study on the LRH approach, and drawn comparisons between LRH and the Banerjee&Mukherjee approach [23] via experiments over randomly generated networks. Given the total number of nodes, say *n*, the greatest possible number of bi-directional links is $C(n,2)$, where *C* is the combination operation. Then, for a network with *n* nodes and connectivity *v*, it is generated by randomly selecting $C(n,2)\times v$ out of the $C(n,2)$ bi-directional links of the network. In the experiments, we used 32 wavelengths on each fiber link (i.e., $|W|$=32) for all networks.

Accordingly in the experiment, we considered the random network, as shown in Figure 6(a). Random network consists of 11 nodes including 2 FSC (nodes 1-2) or 4 FSC (nodes 1-4) nodes, and 22 bi-directional links, corresponding to a connectivity (*v*) of 0.4. Results are plotted in Figures 6(b) and 6(c).

In the computation using our LRH approach, we adopted QT=50 and three different termination criteria. The two criteria are: Iteration_Number =1000, 2000. The algorithm was written in the C language and operated on a PC running Windows XP with a 2.53GHz CPU power. In the LPR-based method, by

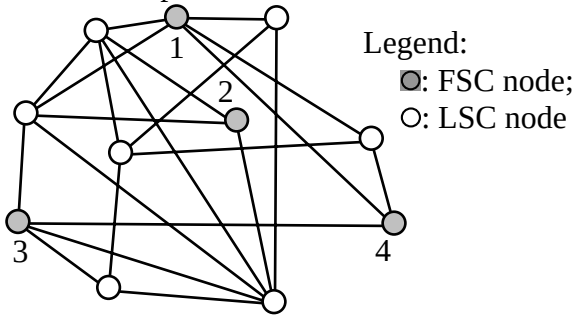

(a) Network topology

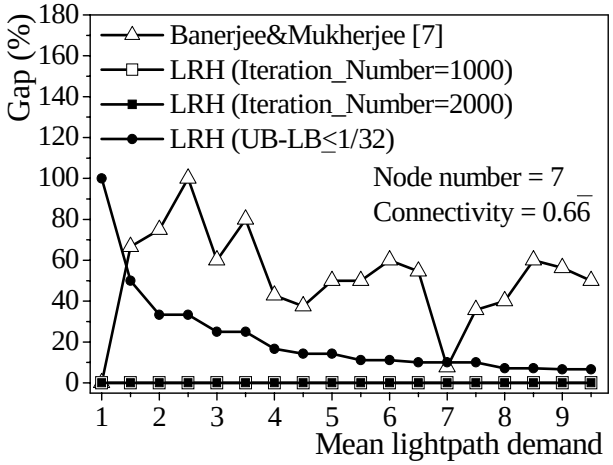

(b) Accuracy for NET

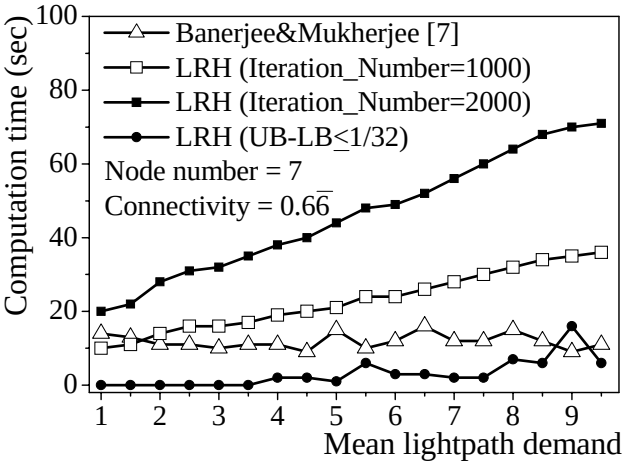

(c) Computation time for NET

Figure 6. Comparisons of accuracy and computation time for random network.

removing Constraints (7) and (9), the original Integer Linear Programming (ILP) problem is relaxed to a Linear Programming (LP) problem. Thus, the solution to the relaxed problem is a legitimate lower bound of the original ILP problem. The upper bound is then obtained according to the randomization procedure proposed in [23]. In the experiment, the LP problem was solved using the *CPLEX* software, operating in the same PC environment. For both approaches, the accuracy is measured in terms of the Gap(%) which is defined as the ratio of the difference of the UB and LB values to the LB value in percentage.

For random network with size over 10 nodes as shown in Figure 7, the LPR method yields larger gaps, namely poorer accuracy, and demands exponentially increasing computation time. In contrast, the LRH approach achieves identical lower and upper bounds, namely the optimal solutions under several lightpath demand cases. In fact, we discover that, both LRH and LPR approaches achieve tight lower bounds. Significantly, the LRH heuristic algorithm arrives at much improved upper bounds due to the use of the Lagrangean multipliers derived upon seeking the Lagrangean relaxation solution. It is worth noticing that the results of the LRH approach using the termination requirement are not shown in Figures 7 and 8. This is due to its high accuracy and low computation time, yielding impossible plotting within the figures. Specifically, we discover from Figure 7 that the LRH approach using the 1000 iterations achieves as high accuracy as that using the 2000 iterations under most demand cases.

Furthermore, as shown in Figure 8, the LRH approach outperforms the LPR method in computation time by at least one order of magnitude under all cases. Notice that, the LRH approach using the termination requirement incurs exceptionally low computation times that are equal to (0,1,7,24,18,17,9, 31) for eight lightpath demands, respectively. In this case, compared to the LPR method, the LRH approach offers an improvement of computation time by more than two orders of magnitude.

To observe the performance of our LRH approach

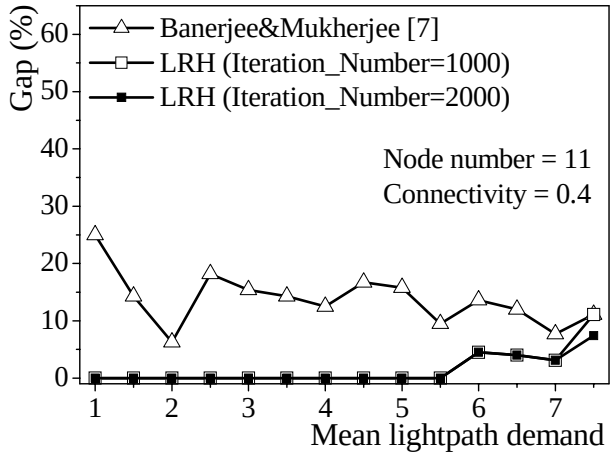

(a) Network with 2 FSC nodes

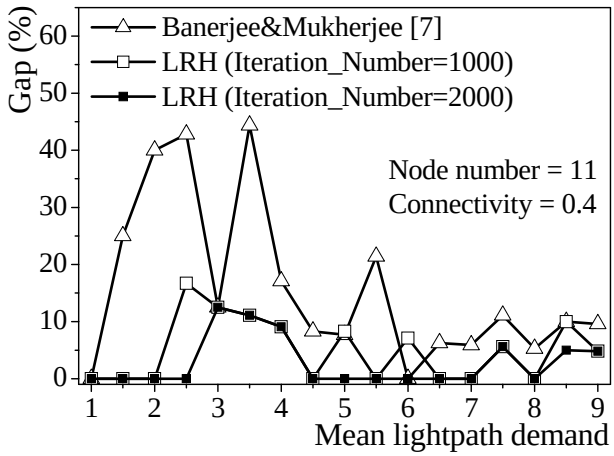

(b) Network with 4 FSC nodes

Figure 7. Comparison of accuracy for random network.

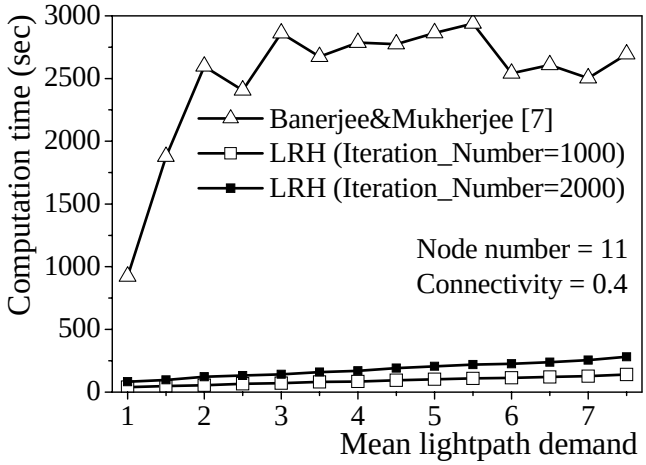

(a) Network with 2 FSC nodes

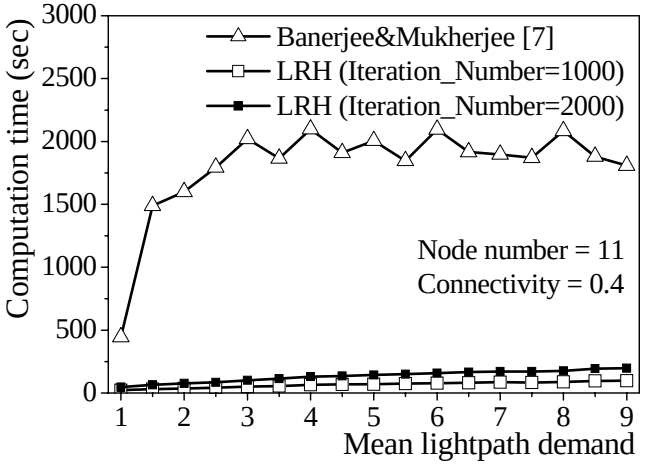

(b) Network with 4 FSC nodes

Figure 8. Comparison of computation time for random network.

for large sized networks, we carried out experiments on two well-known ARPA network, as shown in Figure 9(a). The ARPA network has 61 nodes including 4 FSC nodes and 148 bi-directional links, which corresponds to a connectivity (v) of 0.04. There are 64 wavelengths on each fiber for both networks.

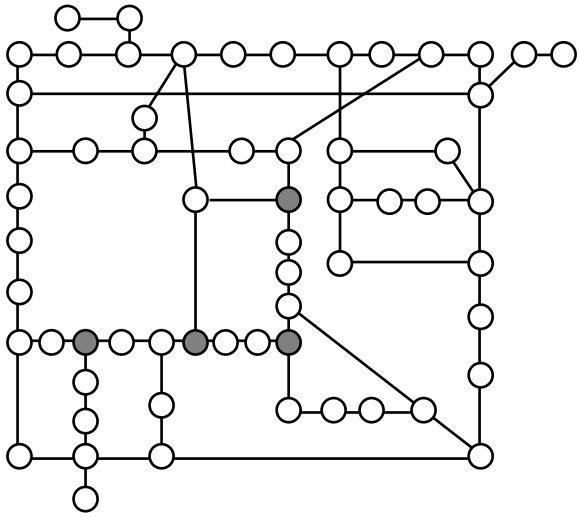

(a) Topology (61 nodes and 148 links)

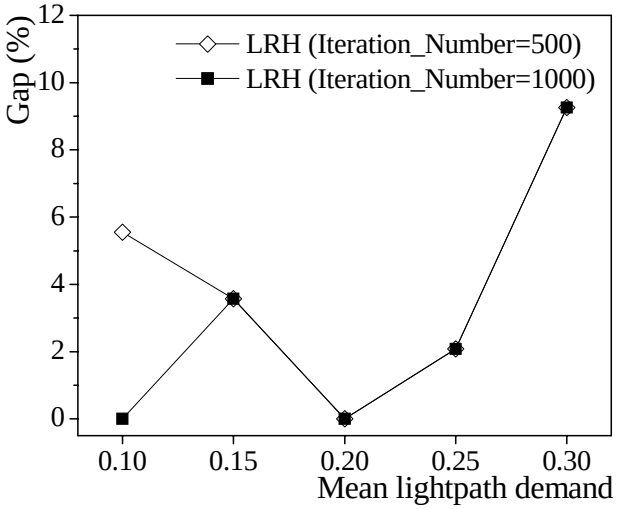

(b) Computation accuracy

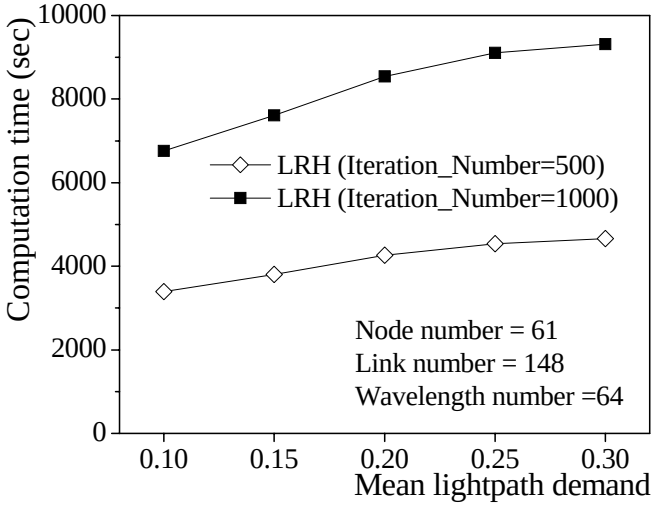

(c) Computation time

Figure 9. The ARPA network and LRH results.

Numerical results are displayed in Figure 9.

In the experiment, we adopted QT=50 and two different termination criteria, namely Iteration_Number=500 and 1000. For the USA network, LRH achieves a guarantee of no more than 8% Gap between the upper and lower bounds under both termination criteria. For the ARPA network, the LRH achieves a guarantee of no more than 9.3% Gap in less than 9400 sec computation time. We particularly observe from Figure 9(c) that the accuracy of the LRH approach based on the 500-iteration termination criterion is as high as that based on the 1000-iteration termination criterion under most lightpath demand cases. This again demonstrates the superiority of the LRH approach to the RWA$^+$ problem with respect to both computation accuracy and time complexity for large sized networks.

4.3 Optical Metro Ring Network

4.3.1 Network and Node Architectures

Nodes in HOPSMAN are interconnected via a single unidirectional fiber that carries multiple WDM data channels (λ_1-λ_W,10-Gb/s) and one control channel (λ_0, 2.5-Gb/s) containing the status of data channels. Channels are further divided into synchronous time slots. Nodes are equipped with one fixed transmitter/receiver for accessing the control channel; and one or multiple tunable transmitter(s)/ receiver(s) for dropping/adding packets from/to data channels on a slot basis.

HOPSMAN has three types of nodes- POP-node (P-node), Ordinary-node (O-node), and Server-node (S-node). A P-node is a gateway between HOPSMAN and long-haul networks, and typically includes multiple tunable transmitters/receivers. An O-node is a regular node with one tunable transmitter/receiver. Finally, an S-node is an O-node but additionally equipped with a slot-eraser device, making bandwidth reusable and thus achieving greater bandwidth efficiency. Notice revealed by our study that, bandwidth efficiency improves greatly with only a few S-nodes in a network.

The node architecture is shown in Figure 10. First, a fixed optical drop filter extracts the control channel information. In coordination with the SYNC Monitoring Module, the Channel Timing Processor is responsible to identify the beginning of a control/data slot. Notice that, the slot boundaries of the control and data channels are aligned during transmissions. With

status of data channels, the MAC Processor mainly performs the MAC scheme, namely the determination of the add/drop/erase operations and the status updates of the associated control channel mini-slots.

The add/drop of data channel packets operates under the broadcast-and-select configuration. With wideband optical splitters/couplers, the node receives/ transmits packets by tuning the tunable receiver/ transmitter to the target wavelength. Finally, the updated control channel slot signal is transmitted via the fixed transmitter and combined with data channel slots via the optical add filter (OAF).

4.3.2 Medium Access Control (MAC)

Essentially, the MAC scheme schedules a quota with credit-window access per *cycle* basis. A cycle is composed of a pre-determined, fixed number of slots. Within each cycle, each node is permitted to transmit a maximum number of packets (slots), called quota. In addition, if a node has fewer packets to transmit than its quota in a cycle, the node yields the unused bandwidth (slots) to downstream nodes. In return, the node receives the same number of slots as credits. Such credits allow the node to transmit more packets (than its quota) in future cycles within the window, which is the maximum number of cycles before credits expire.

To this end, each control slot contains a header, followed by *W* number of destination/status mini-slots corresponding to *W* wavelengths (slots), respectively. There are four different statuses for data slots- IDLE, BUSY, READ, and MRKD. A node wishing to transmit and seeing an IDLE slot transmits a packet and modifies the status to BUSY. A node that has dropped a packet from the ring updates the status to READ, allowing the next encountered S-node to erase the corresponding slot resulting in slot reuse by downstream nodes. Finally, a node alters from IDLE to MRKD for unused bandwidth. At later time, the node can use an extra slot (beyond the quota) should it have a credit and there exist a MRKD slot.

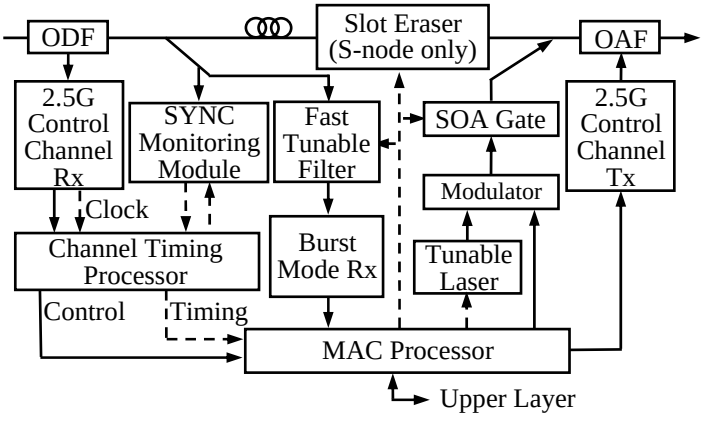

Figure 10. Optical node architecture.

Simulation results (Figures 11(a) and 11(b)) demonstrate that the MAC scheme enables high bandwidth efficiency and fair bandwidth allocation under heavy loads while serving simple random access (low delay) under light loads. Notice that HOPSMAN achieves a throughput of nearly one (0.96) with only two S-nodes in the network. Moreover, as shown in Figure 11(c), the scheme satisfies an acceptable grade of access delay for high-burstiness

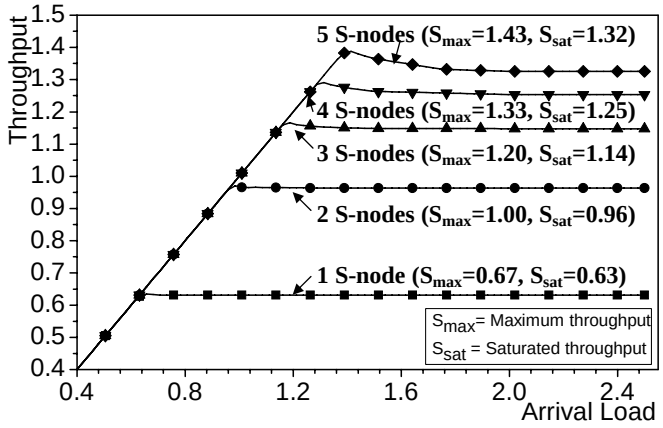

(a) Throguhput under different S-node numbers

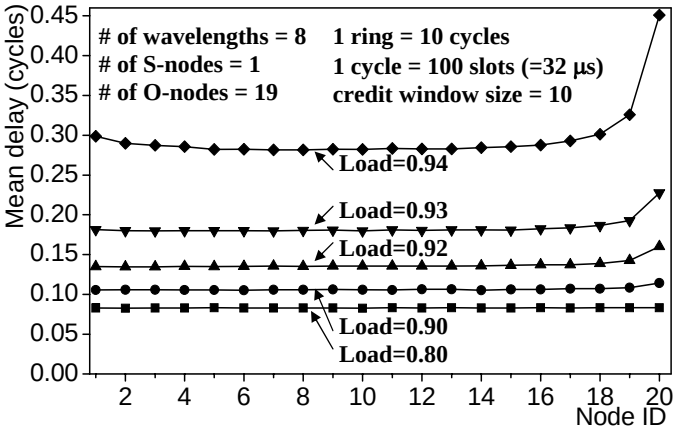

(b) Access fairness under different loads

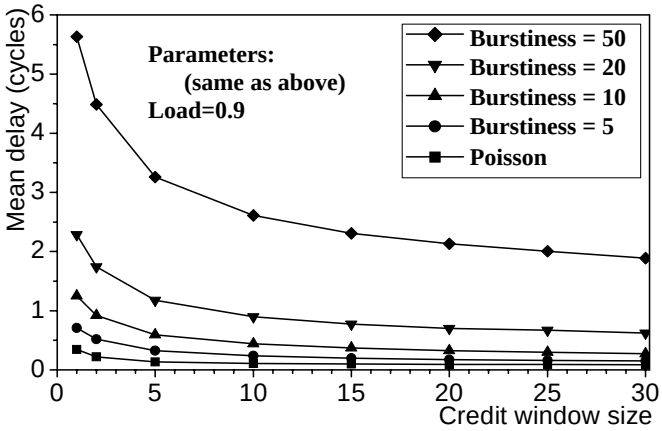

(c) Credit window size effect on access delay

Figure 11. HOPSMAN simulation results.

traffic by dynamically adjusting the credit window size.

4.3.3 Experimentation and Results

We constructed an experimental ring testbed for HOPSMAN. The ring is 38.3 km long (500 time slots, 50 slots/cycle, and 320 ns/slot), and includes two O-nodes and one S-node. The testbed uses four data channels on wavelengths at 1551.72nm, 1553.33nm, 1554.94nm and 1556.55nm; and a control channel on wavelength at 1540.56nm. The input and output powers per channel are kept at -10dBm and 0dBm, respectively, by attenuators and amplifiers on the ring.

Within the S-node (Figure 12(a)), besides the MAC processor, the node is equipped with a network processor and Ethernet interface, including a 2.5-Gb/s burst mode receiver (BMR), to establish real network connectivity and display video packets. Notice that, due to unavailability of higher speed BMRs, each data channel is downgraded to 2.5 Gb/s in the testbed. The MAC and network processors were implemented via Xilinx Vertex-II and Spartan3 FPGA chips, respectively. The slot eraser was constructed via a pair of Mux/Demux and an array of SOA gates, which can be on/off turned in 5 ns.

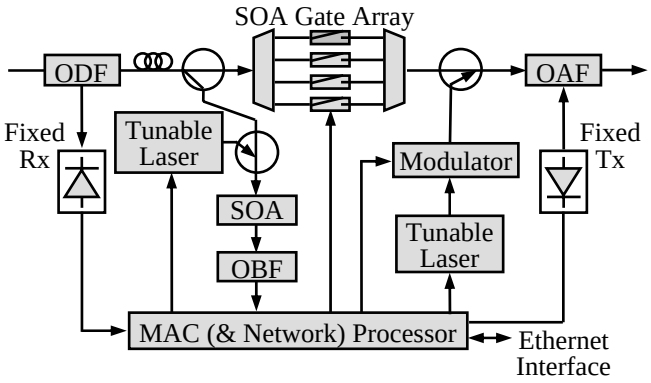

(a) Experimental setup for S-node

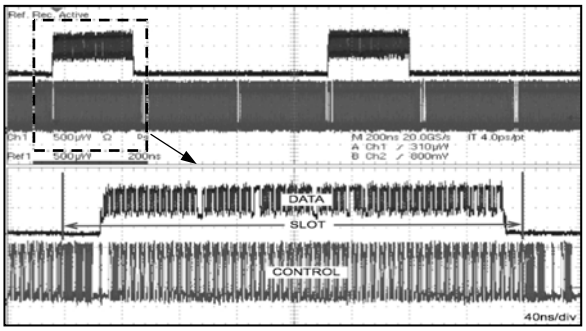

(b) Synchronized ata and control slots

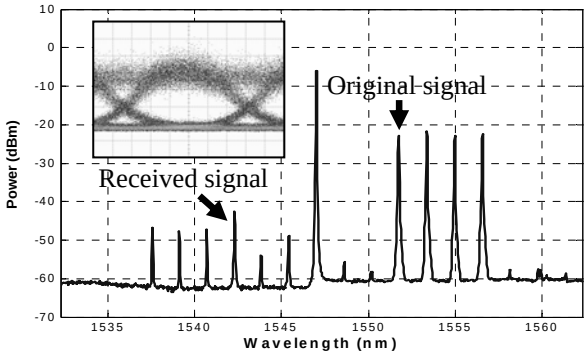

(c) Optical spectrum of wavelength convertion by four-wave-mixing based filter

Figure 12. Experimental setup and results.

First, the boundaries of the data and control slots were fully synchronized as shown in Figure 12(b). Besides, the node used a tunable receiver to extract signal from one of four wavelengths through a four-wave-mixing based filter. Via a tunable laser and SOA, the chosen data wavelength was converted to the wavelength of the fixed filter (Figure 12(c)), with 18dB conversion efficiency. The output channel's eye diagram is shown in Figure 12(c). Finally, to inject data packets to the ring, we adopted an SG-DBR tunable laser with 40ns tuning delay, resulting in a guard time between data packets being set as 40ns. Above results demonstrate the viability and superiority of HOPSMAN.

Reference

[1] B. Mukherjee, "WDM Optical Communication Networks: Progress and Challenges," *IEEE J. Select. Areas Commun.*, vol. 18, no. 10, Oct. 2000, pp. 1810-1824.

[2] M. Herzog, et al., "Metropolitan Area Packet-Switched WDM Networks: A Survey on Ring Systems," *IEEE Commun. Surveys & Tutorials*, vol. 6 2004, pp. 2-20.

[3] F. Callegati, G. Corazza, and C. Raffaelli, "Exploitation of DWDM for Optical Packet Switching with Quality of Service Guarantees," *IEEE J. Select. Areas Commun.*, vol. 20, no. 1, Jan. 2002, pp. 190-201.

[4] L. Xu, H. Perros, and G. Rouskas, "Techniques for Optical Packet Switching and Optical Burst Switching," *IEEE Comm. Mag.*, vol. 39, no. 1, Jan. 2001, pp. 136-142.

[5] L. Xu, H. Perros, and G. Rouskas, "The Perspective of Optical Packet Switching in IP Dominant Backbone and Metropolitan Networks," *IEEE Comm. Mag.*, vol. 39, no. 3, March 2001, pp. 136-141.

[6] D. Hunter, *et al*., "SLOB: A switch With Large Optical Buffers for Packet Switching," *Journal*

of Lightwave Technology, vol. 16, no. 10, Oct. 1998, pp. 1725-1736.

[7] T. Battestilli, and H. Perros, "An Introduction to Optical Burst Switching," *IEEE Comm. Mag.*, vol. 41, no. 8, Aug. 2003, pp. S10-S15.

[8] M. Yoo, C. Qiao, and S. Dixit, "Optical Burst Switching for Service Differentiation in the Next Generation Optical Internet," *IEEE Comm. Mag.*, vol. 39, no. 2, Feb. 2001, pp. 98-104.

[9] V. Vokkarane, and J. Jue, "Prioritized Burst Segmentation and Composite Burst-Assembly Techniques for QoS Support in Optical Burst-Switched Networks," *IEEE J. Select. Areas Commun.*, vol. 21, no. 7, Sep. 2003, pp. 1198-1209.

[10] J. Wei, and R. McFarland, "Just-In-Time Signaling for WDM Optical Burst Switching Networks," *Journal of Lightwave Technology*, vol. 18, no. 12, Dec. 2000, pp. 2019-2037.

[11] Y. Xiong, M. Vandenhoute, and H. Cankaya, "Control Architecture in Optical Burst-Switched WDM Networks," *IEEE J. Select. Areas Commun.*, vol. 18, no. 10, Oct. 2000, pp. 1838-1851.

[12] M. Yoo, C. Qiao, and S. Dixit, "QoS Performance of Optical Burst Switching in IP-over-WDM Networks," *IEEE J. Select. Areas Commun.*, vol. 18, no. 10, Oct. 2000, pp. 2062-2071.

[13] M. Yuang, J. Shih, and P. Tien, "Traffic Shaping for IP-over-WDM Networks based on Optical Coarse Packet Switching Paradigm," in *Proc. European Conference on Optical Communication (ECOC)*, 2003.

[14] M. Yuang, S. Lee, P. Tien, Y. Lin, J. Shih, F. Tsai, and A. Chen, "Optical Coarse Packet-Switched IP-over-WDM Network (OPSINET): Technologies and Experiments," *IEEE Journal on Selected Areas in Communications*, vol. 24, no. 8, Aug. 2006.

[15] E. Mannie, *et al.*, "Generalized Multi-Protocol Label Switching (GMPLS) Architecture," draft-ietf-ccamp-gmpls-architecture-03.txt, Feb. 2003, work in progress.

[16] L. Yang, Y. Jiang, and S. Jiang, "A Probabilistic Preemptive Scheme for Providing Service Differentiation in OBS Networks," in *Proc. IEEE GLOBECOM*, 2003.

[17] H. Harai, M. Murata, and H. Miyahara, "Performance analysis of wavelength assignment policies in all-optical networks with limited-range wavelength conversion," *IEEE J. Select. Areas Commun.*, vol. 16, no. 7, Sep. 1998, pp. 1051-1060.

[18] R. Ramaswami, and K. Sivarajan, *Optical Networks- A Practical Perspective*, 2nd Edition, Morgan Kaufmann, 2002.

[19] B. Mukherjee, *Optical Communication Networks*, McGraw-Hill, 1997.

[20] R. Ramaswami, and G. Sasaki, "Multiwavelength Optical Networks with Limited Wavelength Conversion," *IEEE/ACM Trans. Networking*, vol. 6, no. 6, Dec. 1998, pp. 744-754.

[21] P. Ho, and H. Mouftah, "Routing and Wavelength Assignment with Multigranularity Traffic in Optical Networks," *Journal of Lightwave Technology*, vol. 20, no. 8, Aug. 2002, pp. 1292-1303.

[22] K. Zhu, H. Zhu, and B. Mukherjee, "Traffic Engineering in Multigranularity Heterogeneous Optical WDM Mesh Networks Through Dynamic Traffic Grooming," *IEEE Networks*, vol. 17, no. 2, March/April 2003, pp. 8-15.

[23] D. Banerjee, and B. Mukherjee, "A Practical Approach for Routing and Wavelength Assignment in Large Wavelength-Routed Optical Networks," *IEEE J. Select. Areas Commun.*, vol. 14, no. 5, Sep. 1996, pp. 903-908.

[24] C. Xiaowen, L. Bo, and I. Chlamtac, "Wavelength Converter Placement under Different RWA Algorithms in Wavelength-Routed All-Optical Networks," *IEEE Trans. Commun.*, vol. 51, no. 4, April 2003, pp. 607-617.

[25] H. Qin, S. Zhang, and Z. Liu, "Dynamic Routing and Wavelength Assignment for Limited-Range Wavelength Conversion," *IEEE Commun. Letters*, vol. 7, no. 3, March 2003, pp. 136-138.

[26] A. Mokhtar, and M. Azizoglu, "Adaptive Wavelength Routing in All-Optical Networks," *IEEE/ACM Trans. Networking*, vol. 6, no. 2, April 1998, pp. 197-206.

[27] B. Gavish, P. Trudeau, M. Dror, M. Gendreau, and L. Mason, "Fiberoptic Circuit Network Design under Reliability Constraints," *IEEE J.*

Select. Areas Commun., vol. 7, no. 8, Oct. 1989, pp. 1181-1187.

[28] H. Chen, C. Chu, and J. Proth, "An Improvement of The Lagrangean Relaxation Approach for Job Shop Scheduling: A Dynamic Programming Method," *IEEE Trans. Robotics and Automation*, vol. 14, no. 5, Oct. 1998, pp. 786 -795.

[29] M. Guignard, "On Solving Structured Integer Programming Problems with Lagrangean Relaxation and/or Decomposition," in *Proc. IEEE Decision and Control*, Dec. 1989, pp. 1136 -1141.

[30] R. Ahuja, T. Magnanti, and J. Orlin, *Network Flows: Theory, Algorithms, and Applications*, Prentice-Hall, 1993.

[31] M. Saad, and Z. Luo, "A Lagrangean Decomposition Approach for the Routing and Wavelength Assignment in Multifiber WDM Networks", in *Proc. IEEE GLOBECOM '02*, pp. 2818-2822.

[32] Y. Zhang, O. Yang, and H. Liu, "A Lagrangean Relaxation Approach to the Maximizing-Number- Of-Connection Problem in WDM Networks," in *Proc. IEEE Workshop on High Performance Switching and Routing*, 2003.

[33] I.M. White, M. S. Rogge, K. Shrikhande, and L. G. Kazovsky, "A Summary of the HORNET Project: A Next-Generation Metropolitan Area Network," *IEEE Journal on Selected Areas in Communications*, vol. 21, no. 9, Nov. 2003, pp. 1478-1494.

[34] L. Dittmann, et. al., "The European IST Project DAVID: A Viable Approach Toward Optical Packet Switching," *IEEE Journal on Selected Areas in Communications*, vol. 21, no. 7, Sept. 2003, pp. 1026-1040.

[35] A. Carena, et. al., "RingO: An Experimental WDM Optical Packet Network for Metro Applications," *IEEE Journal on Selected Areas in Communications*, vol. 22, no. 8, Oct. 2004, pp. 1561-1571.

[36] M. A. Marsan, et. al., "All-Optical WDM Multi-Rings with Differentiated QoS," *IEEE Comm. Mag.*, vol. 37, no. 2, Feb. 1999, pp. 58-66.

[37] J. Cai, A. Fumagalli, and I. Chlamtac, "The Multitoken Interarrival Time (MTIT) Access Protocol for Supporting Variable Size Packets over WDM Ring Network," *IEEE Journal on Selected Areas in Communications*, vol. 18, no. 10, Oct. 2000, pp. 2094-2104.

[38] C. S. Jelge and J. M. H. Elmirghani, "Photonic Packet WDM Ring Networks Architecture and Performance," *IEEE Comm. Mag.*, vol. 40, no. 11, Nov. 2002, pp. 110-115.

五、計畫成果自評

In this final report, we first propose a dual-purpose, delay and loss QoS-enhanced traffic control scheme, called (ψ,τ)-Scheduler/Shaper, exerted at ingress nodes for OCPS IP-over-WDM networks. Providing delay class differentiation, (ψ,τ)-Scheduler assures each weight-based delay class a stochastic 99% delay bound obtained from simulation results. In addition, (ψ,τ)-Shaper provides loss class differentiation by means of assigning larger burst sizes to higher priority classes. We have performed simulations on an ARPANET network to make loss performance comparisons between the OCPS with (ψ,τ)-Shaper and the Just-Enough-Time (JET)-based OBS networks. Simulation results demonstrated that, due to the near-far problem, OBS undergoes several orders of magnitude increase in packet loss probability for Class *H* traffic particularly under a smaller burst size. As opposed to OBS, the in-band-controlled-based OCPS network was shown to provide invariably superior packet loss performance for a high priority traffic class, enabling effective facilitation of loss class differentiation.

In the second year, we have resolved a RWA^{+} problem using the LRH method, which is a Lagrangean Relaxation based approach augmented with an efficient primal heuristic algorithm. With the aid of generated Lagrangean multipliers and lower bound indexes, the primal heuristic algorithm of LRH achieves a near-optimal upper-bound solution. A performance study delineated that the performance trade-off between accuracy and convergence speed can be manipulated via adjusting the Quiescence Threshold parameter in the algorithm. We have drawn comparisons of accuracy and computation time between LRH and the Linear Programming Relaxation (LPR)-based method, under random network. Experimental results demonstrated that, particularly for small to medium sized networks, the LRH approach using a termination requirement profoundly outperforms the LPR method and fixed-iteration-based LRH, in both accuracy and

computational time complexity. Furthermore, for large sized networks, i.e., the ARPA network, numerical results showed that LRH achieves a near optimal solution within acceptable computation time. The above numerical results justify that the LRH approach can be used as a dynamic RWA^+ algorithm for small to medium sized networks, and as a static RWA^+ algorithm for large sized networks.

In the last year, we have proposed a high-performance optical packet-switched metro WDM ring network, called HOPSMAN. Equipped with novel medium access control, HOPSMAN provides bandwidth efficiency, access delay, fairness, and bursty traffic adaptation. We have performed simulations on a ring network with three types of nodes. Simulation results demonstrate that the MAC scheme enables high bandwidth efficiency and fair bandwidth allocation under heavy loads. We also constructed an experimental ring testbed to demonstrate the viability and superiority of HOPSMAN.

However, the real networks face the different type of service, such as voice, video, and data. We must design a QoS-enhenced metro ring network to support the real traffic data. In addition, we could consider the benefit of bandwidth reuse in the ring topology network. In the next three-year project, we will concentrate on design, analysis, and testbed construction of optical WDM QoS-Enabled metro ring network.

The complete version of the final report has been published in the following.

1. 施汝霖 [2006 July], 博士論文：全光近屬封包交換 IP-over-WDM 網路之訊務控制技術與效能分析 (Traffic Control and Performance Analyses for Optical Coarse Packet-Switched IP-over-WDM Networks)
2. M. Yuang, P. Tien, J. Shih, and A. Chen, "QoS Scheduler/Shaper for Optical Coarse Packet Switching IP-over-WDM Networks," *IEEE Journal on Selected Areas in Communications*, vol. 22, no. 9, Nov. 2004
3. M. Yuang, S. Lee, P. Tien, Y. Lin, J. Shih, F. Tsai, and A. Chen, "Optical Coarse Packet-Switched IP-over-WDM Network (OPSINET): Technologies and Experiments," *IEEE Journal on Selected Areas in Communications*, vol. 24, no. 8, Aug. 2006.
4. S. Lee, M. Yuang, P. Tien and S. Lin, "A Lagrangean relaxation-based approach for routing and wavelegth assignment in multigranularity optical WDM networks," *IEEE Journal on Selected Areas in Communications*, vol. 22, no. 9, Nov. 2004.
5. M. Yuang, S. Lee, B. Lo, I. Chao, Y. Lin, P. Tien, C. Chien and J. Chen, "HOPSMAN: An Experimental Optical Packet-Switched Metro WDM Ring Network with High-Performance Medium Access Control," *IEEE ECOC'06*.